PCCP

Palladium cluster complex $[Pd_{13}(\mu_4\text{-}C_7H_7)_6]^{2+}$ (C_7H_7 = Tropylium) with fcc-close-packed cuboctahedral Pd_{13} core and isomers: Theoretical insight into ligand-control of Pd_{13} core structure

Journal:	*Physical Chemistry Chemical Physics*
Manuscript ID	CP-ART-07-2023-003262.R1
Article Type:	Paper
Date Submitted by the Author:	25-Aug-2023
Complete List of Authors:	Zhu, Bo; Northeast Normal University,, Institute of Functional Material Chemistry, Key Laboratory of Polyoxometalate Science of Ministry of Education, Faculty of Chemistry Murahashi, Tetsuro; Tokyo Institute of Technology, Department of Chemical Science and Engineering Sakaki, Shigeyoshi; Kyoto University, Fukui Institute for Fundamental Chemistry

PCCP

PAPER

Palladium cluster complex $[Pd_{13}(\mu_4\text{-}C_7H_7)_6]^{2+}$ (C_7H_7 = Tropylium) with *fcc*-close-packed cuboctahedral Pd_{13} core and isomers: Theoretical insight into ligand-control of Pd_{13} core structure

Received 00th January 20xx,
Accepted 00th January 20xx

DOI: 10.1039/x0xx00000x

Bo Zhu,[a] Tetsuro Murahashi,*[b] and Shigeyoshi Sakaki*[c]

One of challenging targets in today's chemistry is size-, shape-, and metal-atom packing-controlled synthesis of nano-scale transition metal cluster complexes because key factors governing these features have been elusive. Here, we present a DFT study on a recently synthesized palladium cluster complex $[Pd_{13}(\mu_4\text{-}C_7H_7)_6]^{2+}$ (named **Cubo-μ4**; C_7H_7 = tropylium) with an *fcc*-close-packed cuboctahedral Pd_{13} core and possible isomers. The stability decreases in the order **Cubo-μ4** > $[Pd_{13}(\mu_3\text{-}C_7H_7)_3(\mu_4\text{-}C_7H_7)_3]^{2+}$ with an *hcp*-close-packed anticuboctahedral Pd_{13} core (**Anti-μ3,4**) > $[Pd_{13}(\mu_3\text{-}C_7H_7)_6]^{2+}$ with a *non*-close packed icosahedral Pd_{13} core (**Ih-μ3**) > $[Pd_{13}(\mu_4\text{-}C_7H_7)_6]^{2+}$ with an anticuboctahedral Pd_{13} core (**Anti-μ4**) > $[Pd_{13}(\mu_3\text{-}C_7H_7)_6]^{2+}$ with a cuboctahedral Pd_{13} core (**Cubo-μ3**). This ordering disagrees with the stability of the Pd_{13} core. The key factor governing the stability and metal-atom packing manner of these Pd_{13} cluster complexes is not the stability of the Pd_{13} core but the interaction energy between the Pd_{13} core and the $[(C_7H_7)_6]^{2+}$ ligand shell. The interaction energy is mainly determined by the charge-transfer from the Pd_{13} core to the $[(C_7H_7)_6]^{2+}$ ligand shell and the coordination mode of the C_7H_7 ligand (μ_3- vs μ_4-coordination bond). In the μ_4-coordination, all seven C atoms of the C_7H_7 ligand interact with four Pd atoms of the Pd_4 plane using two C=C doble bonds and one π-allyl moiety. On the other hand, in the μ_3-coordination, one or two C atoms of the C_7H_7 cannot form bonding interaction with Pd atom of the Pd_3 plane. Thus, the use of apropriate capping ligands is one of the key points in synthesis of nano-scale metal cluster complexes.

Introduction

Size-, shape-, and metal-atom packing-controlled synthesis of nano-scale metal clusters/particles is one of extremely important research topics in today's chemistry since physical properties, reactivity, and catalysis are highly dependent on the size, shape, and metal-atom packing manner of metal clusters/particles, as reviewed recently.[1-4] Such synthesis is still challenging even nowadays because the key factors governing the structure of metal clusters/particles have been elusive.

It is well known that many transition metal cluster complexes with carbonyl ligands have been reported.[5,6] In metal cluster complexes consisting of more than ten metal atoms, however, it is not easy to find important factors governing the size, shape and packing manner of metal atoms. This is true because there are many factors to consider. In addition, since the carbonyl forms strong coordination bond with various metal atoms at various coordination sites, it is unlikely that carbonyl ligand can control structures of metal-cluster complexes. The use of cyclic π electron molecules as ligands could solve some problems, since the cyclic π electron molecules can use their molecular planes to control a structure of metal core. However, only a few pioneering studies have succeeded in synthesizing metal cluster complexes with symmetrical structure using cyclic π electron ligands: One example is a nickel cluster complex consisting of an octahedral Ni_6 core and six cyclopentadienyl (Cp) ligands.[7,8] Another one is a ruthenium hydride cluster complex consisting of a trigonal bipyramidal Ru_5 core, four Cp and two pentamethylcyclopentadienyl (Cp*) ligands.[9] These metal cluster complexes have a highly symmetrical structure. However, these metal cluster complexes are much smaller than the desired nano-scale metal cluster complexes. These situations illustrate clearly the difficulty in synthesizing nano-scale transition metal cluster complexes with defined size and symmetrical structures using cyclic π electron ligands.

One of the present authors reported a series of palladium (Pd) cluster complexes[10] such as triangle $Pd_{3-n}Pt_n$ (n = 0 to 3) core,[11-15] Pd_5 sheet[16] and Pd_{10} chain[17] sandwiched between two cyclic π electron compounds. However, a larger Pd cluster complex with a three-dimensionally symmetrical structure had not been synthesized for a long time. Recently, the author and coworkers succeeded in synthesizing a nano-scale three-dimensional Pd cluster complex $[Pd_{13}(\mu_4\text{-}C_7H_7)_6]^{2+}$ (C_7H_7 = tropylium) composed of a highly

[a] *Institute of Functional Materials Chemistry, Faculty of Chemistry, Northeast Normal University, Changchun 130024, P. R. China. E-mail: zhub255@nenu.edu.cn.*
[b] *Department of Chemical Science and Engineering, School of Materials and Chemical Technology, Tokyo Institute of Technology, O-okayama, Meguro-ku, Tokyo 152-8552, Japan. E-mail: mura@apc.titech.ac.jp*
[c] *Institute for Integrated Cell-Material Sciences, Rohm Plaza R312, Kyoto University, Kyoto-Daigaku Katsura, Nishikyo-ku, Kyoto 615-8246, Japan. E-mail: sakaki.shigeyoshi.47e@st.kyoto-u.ac.jp.*

‡ *Electronic supplementary information (ESI) available: Optimized Pd-Pd distances (in Å) in $[Pd_{13}(\mu_4\text{-}C_7H_7)_6]^{2+}$ cuboctahedral Pd_{13} core and their comparisons with experimental values, Atomic charge of $[Pd_{13}(\mu_4\text{-}C_7H_7)_6]^{2+}$ with cuboctahedral and anti-cuboctahedral Pd_{13} cores, Frontier orbitals of anti-cuboctahedral Pd_{13} cores, Frontier orbitals of icosahedral Pd_{13} cores, HOMO and LUMO of $[(C_7H_7)_6]^{2+}$ and Hirshfeld charge of each C_7H_7 at the closed shell singlet, Six singly occupied molecular orbitals (SOMOs) of $[(C_7H_7)_6]$ in the septet state, HOMO, HOMO-1, HOMO-2 of cuboctahedral and anti-cuboctahedral Pd_{13} clusters without ligand, comparisons of stabilities of several Pd_{13} cluster complexes, cartesian coordinates of optimized geometries. See DOI: 10.1039/x0xx00000x*

symmetrical face-centred-cubic (*fcc*)-close-packed cuboctahedral Pd_{13} core (abbreviated as cuboctahedral Pd_{13} core hereinafter) and a nearly octahedral ligand-shell, as shown in Scheme 1.[18] To the best of our knowledge, this is the first example of nano-scale Pd cluster complex with a cuboctahedral Pd_{13} core of well-defined size and symmetrical structure. In this complex, the Pd_4 faces of the Pd_{13} core, rather than the Pd_3 faces, coordinate to the C_7H_7 ligands despite the presence of μ_3-coordination bonds between two cyclic π electron ligands and the $Pd_{3-n}Pt_n$ cluster in experimentally isolated $Pd_{3-n}Pt_n$ complexes.[11-15]

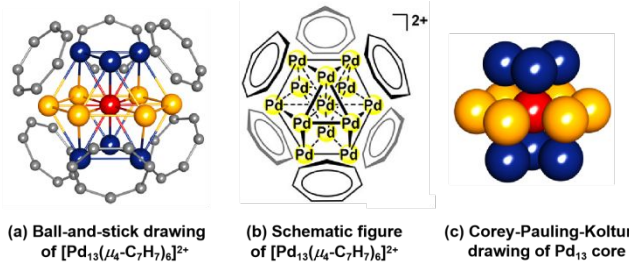

Scheme 1. Experimentally reported structures of $[Pd_{13}(\mu_4\text{-}C_7H_7)_6]^{2+}$ and the Pd_{13} core.[18]

As shown in Fig. 1, the naked M_{13} cluster without ligand has symmetrical structures such as hexagonal close-packed (hcp) anti-cuboctahedral and non-close-packed icosahedral structures in addition to the cuboctahedral structure. The cuboctahedral Pd_{13} cluster can be converted to the anticuboctahedral structure by simply rotating the bottom Pd_3 face by 60°, indicating that the cuboctahedral structure closely resembles the anticuboctahedral one (Figs. 1a and 1b). In these three structures, the icosahedral Pd_{13} cluster is calculated to be the most stable, although the energy difference between them is marginal (Fig. 1). Since the coordination bonds of cyclic π electron ligands are generally considered flexible, one would expect that the stability of the Pd_{13} core determines the structure of $[Pd_{13}(C_7H_7)_6]^{2+}$. If so, we can expect that $[Pd_{13}(\mu_4\text{-}C_7H_7)_6]^{2+}$ complexes with icosahedral and anticuboctahedral Pd_{13} cores are obtained. Therefore, the synthesis of only $[Pd_{13}(\mu_4\text{-}C_7H_7)_6]^{2+}$

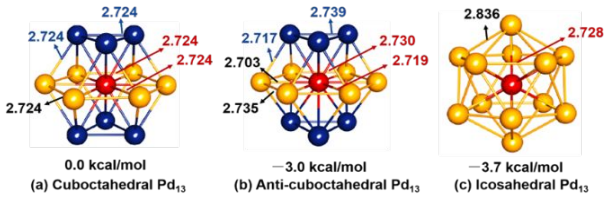

Fig. 1 Three symmetrical structures of Pd_{13} cluster without ligand optimized by DFT calculations at the closed shell singlet state. The value below the structure represents a relative energy (ΔE in kcal/mol) to the cuboctahedral Pd_{13} cluster. Bond distances are presented in angstrom (Å) unit.

with the cuboctahedral Pd_{13} core strongly suggests that there are important factors governing the structure of the Pd_{13} cluster complex. One theoretical study on $[Pd_{13}(\mu_4\text{-}C_7H_7)_6]^{2+}$ with a cuboctahedral Pd_{13} core has been reported,[19] in which orbital interaction has been discussed. However, to the best of our knowledge, key factors governing the structure of metal cluster complex have not been investigated at all either experimentally or theoretically. Lack of the knowledge of such factors is an important obstacle to further developing the chemistry of nano-scale metal cluster complexes.

In order to clarify such important factors, it is necessary to analyse the stability, bonding and electronic structure of the above Pd_{13} cluster complex $[Pd_{13}(\mu_4\text{-}C_7H_7)_6]^{2+}$. To understand alkali metal cluster complexes in which ns (n = principle quantum number, 2 to 6) valence electrons are used for metal-metal and metal-ligand bonds, the jellium model (or super-atom model) has been proposed.[20,21] This model is often employed in theoretical analysis of gold (Au) cluster complexes because Au atom uses 6s electron in Au-Au and Au-ligand bonds. In the present Pd cluster complex, however, the jellium model does not seem to be useful because not 5s electron but 4d electrons are mainly used for Pd-Pd and Pd-ligand bonds. Besides the jellium model, the polyhedral skeletal electron pair (PSEP) model has been proposed to understand structure and bonding of transition metal cluster complexes.[22-25] However, the number of skeletal electron pairs is the same between $[Pd_{13}(\mu_4\text{-}C_7H_7)_6]^{2+}$ with a cuboctahedral Pd_{13} core and its isomer with an anticuboctahedral Pd_{13} core, suggesting that the PSEP model is not useful for investigating these isomers. Therefore, a different approach must be used to study the stabilities and structures of these nano-scale Pd_{13} cluster complexes.

From these experimental and computational findings, we address several important open questions: (i) Why was $[Pd_{13}(\mu_4\text{-}C_7H_7)_6]^{2+}$ with a cuboctahedral Pd_{13} core obtained but were the isomers with anticuboctahedral and icosahedral Pd_{13} cores not? (ii) What factors govern the structure of the Pd_{13} cluster complex with C_7H_7 ligands? (iii) Why does the C_7H_7 ligand interact with the Pd_4 plane but not with the Pd_3 plane despite many examples[11-15] of μ_3-coordination bond? And, (iv) what analysis method is effective in theoretical study of the Pd cluster complexes and related compounds?

In this work, we have theoretically investigated $[Pd_{13}(\mu_4\text{-}C_7H_7)_6]^{2+}$ with a cuboctahedral Pd_{13} core (named **Cubo-μ4** hereinafter) and its possible isomers such as $[Pd_{13}(\mu_3\text{-}C_7H_7)_6]^{2+}$ with a cuboctahedral Pd_{13} core (named **Cubo-μ3**), $[Pd_{13}(\mu_4\text{-}C_7H_7)_6]^{2+}$ and $[Pd_{13}(\mu_3\text{-}C_7H_7)_3(\mu_4\text{-}C_7H_7)_3]^{2+}$ with an anticuboctahedral Pd_{13} core (named **Anti-μ4** and **Anti-μ3,4**, respectively) and $[Pd_{13}(\mu_3\text{-}C_7H_7)_6]^{2+}$ with an icosahedral Pd_{13} core (named **Ih-μ3**). Through this work, we intended to shed new and clear light to these Pd_{13} cluster complexes, obtain correct answers to the above-mentioned open questions and unveil the key factors governing the structure, stability and metal-atom packing manner of the Pd_{13} core.

Results and discussion

We optimized these Pd_{13} cluster complexes and analysed their stabilities and bonding natures using DFT calculations; computational procedures are described in "Computational details and models" section. We first discuss characteristic features of **Cubo-μ4** and then describe the analysis method used in this work. Next, we compare stability between **Cubo-μ4** and isomers using the analysis method. We focus on the reason why **Cubo-μ4** was

experimentally obtained but the others were not and what is the determination factor governing the structure. Last, we discuss several important comparisons of **Cubo-μ4** with **Anti-m4**, **Cubo-μ3** and **Ih-μ3**.

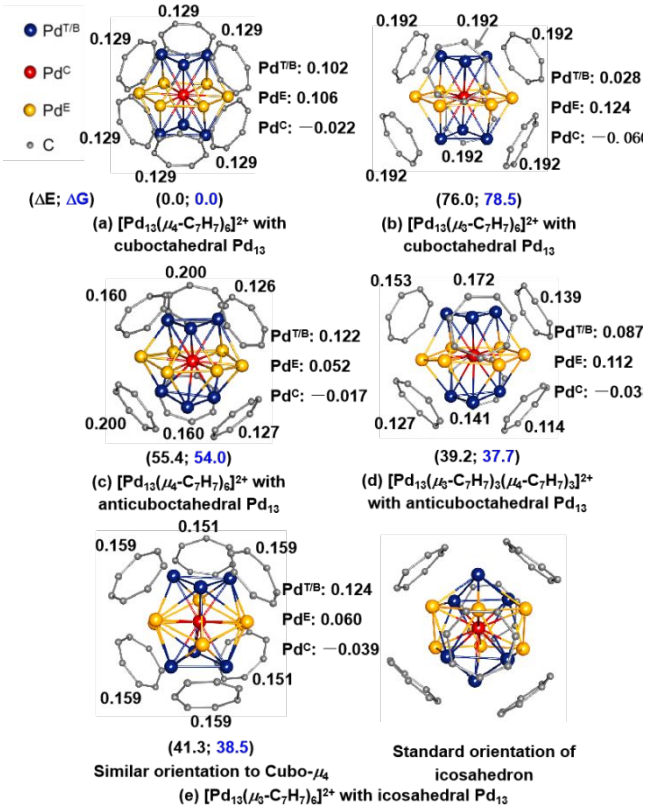

Fig. 2 Optimized geometries and Hirshfeld charges of $[Pd_{13}(\mu_4\text{-}C_7H_7)_6]^{2+}$ with a cuboctaherdal Pd_{13} core (**Cubo-μ4**) (a), $[Pd_{13}(\mu_3\text{-}C_7H_7)_6]^{2+}$ with a cuboctaherdal Pd_{13} core (**Cubo-μ3**) (b), $[Pd_{13}(\mu_4\text{-}C_7H_7)_6]^{2+}$ with an anti-cuboctahedral Pd_{13} core (**Anti-μ4**) (c), $[Pd_{13}(\mu_3,\mu_4\text{-}C_7H_7)_6]^{2+}$ with an anti-cuboctahedral Pd_{13} core (**Anti-μ3,4**) (d), and $[Pd_{13}(\mu_3\text{-}C_7H_7)_6]$ with an icosahedral Pd_{13} core (**Ih-μ3**) (e). Hirshfeld charges of each C_7H_7 ligand and Pd atoms are presented without parentheses (in *e* unit). In parentheses are potential energy and Gibbs energy (in kcal/mol unit) relative to those of **Cubo-μ4**.

Characteristic features of $[Pd_{13}(\mu_4\text{-}C_7H_7)_6]^{2+}$ with a cuboctahedral Pd_{13} core (Cubo-μ4). The optimized structure has a nearly cuboctahedral Pd_{13} core, as shown in Fig. 2a. If **Cubo-μ4** has a perfectly cuboctahedral Pd_{13} core, all of the surface Pd atoms (named Pd^S hereinafter) and all the Pd-Pd distances are equivalent to each other. However, the structure of the Pd_{13} core moderately distorts from the perfectly cuboctahedral structure in both the experimental and optimized geometries: For instance, the difference between the longest and the shortest Pd-Pd distances is 0.106 Å in the experimental geometry[18] and 0.148 Å in the optimized one;§ details of the optimized geometry are presented in Table S1 of the Electronic Supplementary Information (ESI). Considering the moderately distorted structure, the Pd atoms in the equatorial plane and the top and bottom Pd_3 planes are named Pd^E and $Pd^{T/B}$, respectively, to distinguish them, and also the centre Pd atom is named Pd^C hereinafter: They are shown in different colours in Fig. 2.

The Pd^C atom is negatively charged (−0.022 *e* in the Hirshfeld charge[27]) but the Pd^S atom is positively charged (+0.102 *e* and +0.106 e for $Pd^{T/B}$ and Pd^E, respectively), as shown in Fig. 2a: NBO charges[28] in Table S2 of the ESI show the same trend. This trend is found in all the Pd_{13} cluster complexes studied here (Fig. 2), suggesting that this trend is generally observed in the Pd cluster complexes. The negative charge of the Pd^C atom and the positive charge of the Pd^S atom are reasonably explained, as follows: Because the electrostatic potential by thirteen Pd nuclear charges is the largest, the electron density tends to accumulate on the Pd^C atom compared to the Pd^S atom; additional explanation is presented in the footnote §2.

All the C_7H_7 ligands have nearly equal charges (+0.129 *e*), indicating that all C_7H_7 ligands are nearly equivalent. This is consistent with the structure of **Cubo-μ4** possessing six C_7H_7 ligands at nearly octahedral positions.

It should be noted that the averaged value of the Pd^C–$Pd^{T/B}$ and Pd^C–Pd^E Wiberg bond indexes (WBIs)[26] is considerably larger than

Table 1. Pd–Pd distances (R in Å unit) and Wiberg bond indexes (WBIs) of $[Pd_{13}(\mu_4\text{-}C_7H_7)_6]^{2+}$ with a cuboctaherdal Pd_{13} core (**Cubo-μ4**), $[Pd_{13}(\mu_3\text{-}C_7H_7)_6]^{2+}$ with a cuboctaherdal Pd_{13} core (**Cubo-μ3**), $[Pd_{13}(\mu_4\text{-}C_7H_7)_6]^{2+}$ with an anticuboctahedral Pd_{13} core (**Anti-μ4**), $[Pd_{13}(\mu_3\text{-}C_7H_7)_3(\mu_4\text{-}C_7H_7)_3]^{2+}$ with an anticuboctahedral Pd_{13} core (**Anti-μ3,4**), and $[Pd_{13}(\mu_3\text{-}C_7H_7)_6]^{2+}$ with an icosahedral Pd_{13} core (**Ih-μ3**).

	Cubo-μ4		Cubo-μ3		Anti-μ4		Anti-μ3,4		Ih-μ3 [a]	
	R	WBI	R	WBI	R	WBI	R	WBI	R	WBI
Pd^C–$Pd^{T/B}$ [b]	2.765	0.100	2.781	0.105	2.765	0.100	2.781	0.105	2.771	0.102
Pd^C–Pd^E [b]	2.770	0.096	2.761	0.112	2.770	0.096	2.761	0.112	2.700	0.106
Pd^E–$Pd^{T/B}$ [b]	2.762	0.076	2.755	0.107	2.762	0.076	2.755	0.107	2.861	0.086
Pd^E–Pd^E [b]	2.772	0.068	2.762	0.121	2.772	0.068	2.762	0.121	2.829	0.092
$Pd^{T/B}$–$Pd^{T/B}$ [b]	2.777	0.070	2.814	0.083	2.777	0.070	2.814	0.083	-	-
Δ(Pd–Pd) [c]	0.015	0.032	0.059	0.038	0.015	0.032	0.059	0.038	0.161	0.02
(Pd–Pd)av [d]	2.768	0.081	2.772	0.106	2.765	0.100	2.781	0.105	2.771	0.102
R(Pd^C–X) [e]	2.132		2.242		2.230		2.239, 2.115 [f]		2.202	

[a]The Pd_{13} core with an icosahedral structure does not have $Pd^{T/B}$ and Pd^E, strictly speaking. But, we named Pd atoms like those in **Cubo-μ4** and **Cubo-μ3** for comparison; see Fig. 2. [b]The averaged Pd-Pd distance in each group is presented. [c]The difference between the maximum and minimum values. [d]The averaged value of all the Pd-Pd distances. [e]The distance between the centre of Pd_3 plane and the centre of the C_7 ring (named X) of C_7H_7. [f]For μ_3- and μ_4-coordinations, respectively.

those of the Pd^{E}–Pd^{E}, Pd^{E}–$Pd^{T/B}$ and $Pd^{T/B}$–$Pd^{T/B}$ WBIs, as shown in Table 1. These results suggest that the Pd^{C}–Pd^{S} (Pd^{S} = $Pd^{T/B}$ or Pd^{E}) bonds are stronger than the Pd^{S}–Pd^{S} bonds. However, the averaged Pd^{C}–$Pd^{T/B}$ and Pd^{C}–Pd^{E} bond distances differ little from the averaged Pd^{E}–Pd^{E} bond distances (Table 1). In other words, the Pd^{C}–Pd^{S} bond distances differs little from the Pd^{S}–Pd^{S} bond distances despite that the Pd^{C}-Pd^{S} bond is stronger than the Pd^{S}–Pd^{S} bond. This result is not unreasonable because the Pd^{C}–Pd^{S} distances are the same as the Pd^{S}–Pd^{S} distances in the cuboctahedral structure; if the Pd^{C}–Pd^{S} distances shorten according to the large WBI values and the Pd^{S}–Pd^{S} distances lengthen according to the small WBI values, the structure distorts very much from the cuboctahedral one.[§3] It is concluded that the Pd^{C}-Pd^{S} bond is not equivalent to the Pd^{S}-Pd^{S} bond in **Cubo-μ4** even though the bond distance is the same between them.

How to analyse relative stabilities of Cubo-μ4 and isomers. In this work, we analysed relative stabilities of **Cubo-μ4** and isomers using stabilization energies of the Pd_{13} core and the $(C_7H_7)_6$ ligand shell and an interaction energy between them. This analysis method is described in "Computational details and models" section. To apply this method to these Pd_{13} cluster complexes, we explored how we can reasonably separate $[Pd_{13}(C_7H_7)_6]^{2+}$ into the $[Pd_{13}]^{n+}$ core and the $[(C_7H_7)_6]^{(2-n)+}$ ligand shell.

All the C_7H_7 ligands in **Cubo-μ4** have an almost planar geometry, indicating that all the C_7H_7 ligands are understood to be either monocation or neutral radical because both monocation and neutral radical of C_7H_7 have a planar geometry. All the C_7H_7 ligands have a considerably smaller charge (+0.129 *e* in the Hirshfeld charge; Fig. 2) than the formal charge (+1.0 *e*) of the C_7H_7 monocation, suggesting strongly that the C_7H_7 ligand differs from a tropylium cation but is close to a neutral species in **Cubo-μ4**.[§4] Indeed, it is unlikely that C_7H_7 is a monocation in **Cubo-μ4**: If the C_7H_7 ligand is a monocation in **Cubo-μ4**, the Pd_{13} core must have −4.0 *e* charges, which is unreasonable because metal particle tends to have a positive charge but does not a highly negative charge. Thus, we ruled out the understanding that C_7H_7 is a monocation in **Cubo-μ4**. If the Pd_{13} core is neutral, the $(C_7H_7)_6$ ligand shell has +2 charge. This understanding seems reasonable because the C_7H_7 ligand has a positive charge, as shown in Fig. 2; for instance, each C_7H_7 in **Cubo-μ4** has +0.129 *e* in the Hirshfeld charge, which does not differ very much from the charge (+0.333 *e*) of C_7H_7 in the free $[(C_7H_7)_6]^{2+}$ system. Another understanding is that the $(C_7H_7)_6$ moiety is neutral and the Pd_{13} core has +2 charge. This is also reasonable because the metal cluster/particle tends to have a positive charge.

Then, we investigated which of two separation manners, (i) the separation into the neutral Pd_{13} core and the positively charged $[(C_7H_7)_6]^{2+}$ ligand shell and (ii) that into the positively charged $[Pd_{13}]^{2+}$ core and the neutral $[(C_7H_7)_6]$ ligand shell, is reasonable. Cuboctahedral, anticuboctahedral and icosahedral structures of neutral Pd_{13} cluster without ligand were calculated as an equilibrium structure at a closed shell singlet state, as shown in Fig. 1. The cuboctahedral Pd_{13} cluster has triply-degenerated HOMOs and triply-degenerated LUMOs in the closed-shell singlet state, as shown in Scheme 2. These orbital features suggest that when the number of valence electrons decreases or increases, the Pd_{13} core considerably distorts from the cuboctahedral structure due to the Jahn-Teller effect. This means that the neutral Pd_{13} cluster is suitable for a cuboctahedral structure but the $[Pd_{13}]^{2+}$ cluster is not. We also found that the neutral Pd_{13} cluster is suitable for anticuboctahedral and icosahedral structures as an equilibrium structure, as shown by HOMO and LUMO in Schemes S1 and S2 of the ESI.

Next, we explored the electronic structure of the $(C_7H_7)_6$ ligand shell. The neutral $(C_7H_7)_6$ ligand shell composed of six neutral C_7H_7 molecules is reasonable from the viewpoint of the electronic structure of the $(C_7H_7)_6$ moiety. In such a case, however, the Pd_{13} core must have +2 charge, which is already ruled out above. When the Pd_{13} core is neutral in **Cubo-μ4** in a formal sense, the $(C_7H_7)_6$ ligand shell must have +2 charge in a formal sense. To investigate whether the $[(C_7H_7)_6]^{2+}$ ligand shell has a reasonable electronic structure or not, we calculated the $[(C_7H_7)_6]^{2+}$ system at a closed shell singlet state, where the geometry of the $[(C_7H_7)_6]^{2+}$ system was taken to be the same as that in **Cubo-μ4**. This $[(C_7H_7)_6]^{2+}$ system has doubly-degenerated LUMOs and doubly-degenerated HOMOs, as shown in Scheme S3 of the ESI. Six C_7H_7 molecules have almost the same charge (+0.333 *e*), indicating that all C_7H_7 molecules are nearly equivalent in this structure. This feature suggests that six C_7H_7 molecules equivalently contribute to the doubly degenerated HOMO like the e_g orbital of the octahedral molecule. On the basis of these computational results, it is concluded that the ligand shell of **Cubo-μ4** is understood to be a $[(C_7H_7)_6]^{2+}$ system with a closed shell singlet state.

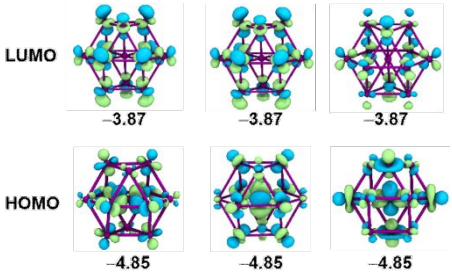

Scheme 2. HOMOs and LUMOs of a cuboctahedral Pd_{13} core, where the geometry was optimized. The number below each MO represents the Kohn-Sham orbital energy (in eV unit).

We address here one open question, whether or not the $[(C_7H_7)_6]^{2+}$ system can have a closed shell singlet ground state when it has the same geometry as that in **Cubo-μ4**. We carefully explored its electronic structure and found that there is no unreasonable feature in the $[(C_7H_7)_6]^{2+}$ ligand shell having the closed shell singlet state when the geometry is taken to be the same as that in **Cubo-μ4**; details are presented in Scheme S4 and page S10 of the ESI.

It is concluded that $[Pd_{13}(C_7H_7)_6]^{2+}$ is reasonably separated into the Pd_{13} core and the $[(C_7H_7)_6]^{2+}$ ligand shell.

Comparison of stability among Cubo-μ4 and isomers. Fig. 2 shows that **Cubo-μ4** is the most stable and the other isomers are much more unstable than **Cubo-μ4**; we could not investigate $[Pd_{13}(\mu_3$-

$C_7H_7)_6]^{2+}$ with an anticuboctahedral Pd_{13} core (named **Anti-μ3**) because this structure changed smoothly to **Anti-μ3,4** during the geometry optimization. Although the success of synthesis depends on kinetic and thermodynamic factors, the extremely larger stability of **Cubo-μ4** than the other isomers is consistent with the experimental finding that **Cubo-μ4** was obtained but the other isomers were not.[18]

As shown in Table 1, the averaged Pd-Pd distance $R(Pd–Pd)_{av}$ increases in the order **Anti-μ4** ~ **Cubo-μ4** < **Ih-μ3** ~ **Cubo-μ3** < **Anti-μ3,4**. This result indicates that **Cubo-μ4** and **Anti-μ4** have the most compact Pd_{13} core. The $R(Pd^C–X)$ distance between the Pd^C atom and the centre (X) of the C_7 ring of the C_7H_7 ligand increases in the order **Cubo-μ4** < **Anti-μ3,4** (average of μ_3- and μ_4-C_7H_7 coordination bonds) < **Ih-μ3** < **Anti-μ4** < **Cubo-μ3**, indicating that the $[(C_7H_7)_6]^{2+}$ ligand shell of **Cubo-μ4** is the most compact. This feature suggests that **Cubo-μ4** has the strongest C_7H_7 coordination bond in these Pd_{13} cluster complexes, which is discussed below.

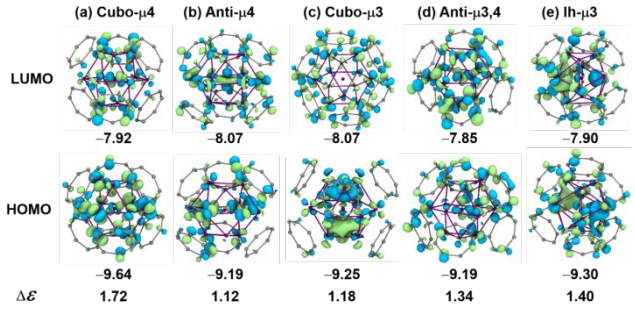

Fig. 3 HOMO and LUMO of $[Pd_{13}(\mu_4\text{-}C_7H_7)_6]^{2+}$ with a cuboctaherdal Pd_{13} core (**Cubo-μ4**) (a), $[Pd_{13}(\mu_3\text{-}C_7H_7)_6]^{2+}$ with a cuboctaherdal Pd_{13} core (**Cubo-μ3**) (b), $[Pd_{13}(\mu_4\text{-}C_7H_7)_6]^{2+}$ with an anticuboctahedral Pd_{13} core (**Anti-μ4**) (c), $[Pd_{13}(\mu_3\text{-}C_7H_7)_3(\mu_4\text{-}C_7H_7)_3]^{2+}$ with an anticuboctahedral Pd_{13} core (**Anti-μ3,4**) (d), and $[Pd_{13}(\mu_3\text{–}C_7H_7)_6]^{2+}$ with an icosahedral Pd_{13} core (**Ih-μ3**) (e). The $\Delta\varepsilon$ is the HOMO-LUMO energy gap (in eV unit).

The HOMO and LUMO of these Pd_{13} cluster complexes mainly consist of Pd d orbitals into which the π* orbitals of the C_7H_7 ligands mix, as shown in Fig. 3. The HOMO-LUMO energy gap decreases in the order **Cubo-μ4** >> **Ih-μ3** > **Anti-μ3,4** > **Cubo-μ3** > **Anti-μ4**. The most stable **Cubo-μ4** has the largest HOMO-LUMO energy gap, suggesting that the interaction between the Pd_{13} core and the $[(C_7H_7)_6]^{2+}$ ligand shell is the strongest in **Cubo-μ4**.

In Table 2, the stabilities of the Pd_{13} core and the $[(C_7H_7)_6]^{2+}$ ligand shell are compared among these isomers. The Pd_{13} core of **Cubo-μ4** is moderately less stable than that of **Ih-μ3** but more stable than in the other isomers. However, the energy difference of the Pd_{13} core between **Cubo-μ4** and the isomers is much smaller than the total energy difference ΔE (Table 2). The stabilization energy of the $[(C_7H_7)_6]^{2+}$ ligand shell in **Cubo-μ4** is less negative than in the isomers (Table 2). However, the difference in the stabilization energy by the $[(C_7H_7)_6]^{2+}$ ligand shell between **Cubo-μ4** and isomers is much smaller than the total energy difference between them (Table 2). On the other hand, the interaction energy E_{int} between the Pd_{13} core and the $[(C_7H_7)_6]^{2+}$ ligand shell significantly differs among these Pd_{13} cluster complexes. The largest (the most negative) E_{int} value is found in **Cubo-μ4** (–687.6 kcal/mol) and then decreases (gets less negative) in the order **Anti-μ3,4** (–646.5 kcal/mol) > **Anti-μ4** (–632.2 kcal/mol) > **Ih-μ3** (–624.9 kcal/mol) > **Cubo-μ3** (–610.1 kcal/mol), where in parenthesis is the E_{int} value and its negative value means a stabilization energy. This decreasing order is the same as that of the relative stability except **Ih-μ3**. In **Ih-μ3**, the E_{int} value (–624.9 kcal/mol) is less negative than in **Anti-μ4** (–632.2 kcal/mol) but **Ih-μ3** is more stable in energy than **Anti-μ4**. This is reasonable because the stabilization energies of the Pd_{13} core (–5.4 kcal/mol) and the $[(C_7H_7)_6]^{2+}$ ligand shell (–16.1 kcal/mol) contribute to the stability of **Ih-μ3** in addition to the E_{int} but these terms compensate with each other and do not contribute at all to the stability of **Anti-μ4** (Table 2).

Table 2. Relative energies (in kcal/mol unit) of $[Pd_{13}(C_7H_7)_6]^{2+}$, Pd_{13} core and $[(C_7H_7)_6]^{2+}$ ligand shell, and the interaction energy (in kcal/mol unit) between Pd_{13} core and $[(C_7H_7)_6]^{2+}$ ligand shell.

Pd_{13}	Name	ΔE [a]	$\Delta E([Pd_{13}]^0)$ [a]	$\Delta E([(C_7H_7)_6]^{2+})$ [a]	E_{int} [b]
Cubo	**Cubo-μ4**	0.0	0.0	0.0	-687.6 (0.0)
	Cubo-μ3	76.0	4.0	-5.4	-610.1 (77.5)
Anti-cubo	**Anti-μ4**	55.4	14.0	-14.0	-632.2 (55.4)
	Anti-μ3,4	39.2	2.4	-4.3	-646.5 (41.1)
Ih	**Ih-μ3**	41.3	-5.4	-16.1	-624.9 (62.7)

[a] ΔE, $\Delta E([Pd_{13}]^0)$, and $\Delta E([(C_7H_7)_6]^{2+})$ represent the differences in total energies of $[Pd_{13}(C_7H_7)_6]^{2+}$, Pd_{13} core and $[(C_7H_7)_6]^{2+}$ ligand shell, respectively. [b] E_{int} means the interaction energy between the Pd_{13} core and the $[(C_7H_7)_6]^{2+}$ ligand shell whose geometries are taken to be the same as those in the $[Pd_{13}(C_7H_7)_6]^{2+}$ complex. In parenthesis represents the difference in E_{int} between **Cubo-μ4** and the others. A positive value means the destabilization energy compared to **Cubo-μ4**.

Even in such **Ih-μ3**, the difference in E_{int} value between **Ih-μ3** and the other isomers is larger than the differences in stabilization energies of the Pd_{13} core and the $[(C_7H_7)_6]^{2+}$ ligand shell (Table 2). Based on these results, it is concluded that the interaction energy E_{int} is the most important factor to determine the stabilities of these cluster complexes.

As described above, each C_7H_7 molecule has a positive charge of +0.333 *e* in the free $[(C_7H_7)_6]^{2+}$ system. Each C_7H_7 ligand in all the isomers of $[Pd_{13}(C_7H_7)_6]^{2+}$ has a smaller positive charge than +0.333 *e*, as shown in Fig. 2, indicating that charge transfer (CT) occurs from the Pd_{13} core to the $[(C_7H_7)_6]^{2+}$ ligand shell. The total charge of the $[(C_7H_7)_6]$ ligand shell increases in the order **Cubo-μ4** (+0.774 *e*) < **Anti-μ3,4** (+0.846 *e*) < **Ih-μ3** (+0.938 *e*) < **Anti-μ4** (+0.973 *e*) < **Cubo-μ3**

(+1.152 *e*), where in parenthesis is the total charge of the $(C_7H_7)_6$ ligand shell. This increasing order is almost the same as the decreasing order of the E_{int} value and the increasing order of the $R(Pd^C–X)$ distance except **Ih-μ3**. These results suggest that the CT from the Pd_{13} core to the $[(C_7H_7)_6]^{2+}$ ligand shell plays important roles to form the bonding interaction between the C_7H_7 ligand and the Pd_{13} core and determine the E_{int} value; in **Ih-μ3**, the E_{int} value is smaller than in **Anti-μ4** despite the smaller total charge of the $(C_7H_7)_6$ ligand shell probably because not the CT but fewer interaction sites is the origin of the weaker μ_3-coordination bond than the μ_4-one, as discussed below.

Comparison between Cubo-μ4 and Anti-μ4. We address here one important open question, why the E_{int} value of **Cubo-μ4** is more negative than those of the other isomers. It is not easy to compare **Cubo-μ4** with **Anti-μ3,4**, because the μ_3-coordination bond of C_7H_7 much differs from the μ_4-one, as discussed below. Therefore, we first compare **Cubo-μ4** with **Anti-μ4** because both have the μ_4-coordination bonds of the C_7H_7 ligands. The E_{int} value is larger (more negative) in **Cubo-μ4** than in **Anti-μ4**, as shown in Table 2. The HOMO-LUMO energy gap is larger (Fig. 3) and the $R(Pd^C–X)$ value is smaller in **Cubo-μ4** than in **Anti-μ4** (Table 1), suggesting that the $[(C_7H_7)_6]^{2+}$ ligand shell more strongly interacts with the Pd_{13} core in **Cubo-μ4** than in **Anti-μ4**. These features are consistent with the larger E_{int} value in **Cubo-μ4** than in **Anti-μ4**. The less positive charge of the C_7H_7 ligand in **Cubo-μ4** than in **Anti-μ4** (Fig. 2) indicates that the CT from the Pd_{13} core to the $[(C_7H_7)_6]^{2+}$ ligand shell occurs more strongly in **Cubo-μ4** than in **Anti-μ4**.

Because it is likely that the HOMO energy of the Pd_{13} core is one of the most important factors in determining the CT interaction between **Cubo-μ4** and **Anti-μ4**, we explored the HOMO energy. The cuboctahedral Pd_{13} cluster has triply-degenerated HOMOs at a higher energy than a non-degenerated HOMO of the anticuboctahedral one, as shown in Fig. 4a.[§5] Therefore, the CT occurs more strongly in **Cubo-μ4** than in **Anti-μ4**.

The next task is to elucidate the reason why the cuboctahedral Pd_{13} core has the HOMOs at a higher energy than does the anticuboctahedral Pd_{13} core. The reason is found in the HOMO feature. In the HOMO of the cuboctahedral Pd_{13} cluster, the d orbital of the Pd^C atom overlaps with the d orbitals of the Pd^S atoms in an antibonding way (Fig. 4b). In the anticuboctahedral Pd_{13} cluster, on the other hand, the d orbital of the Pd^C atom does not participate in the HOMO (Fig. 4b). This difference arises from the difference in symmetry, as follows: The HOMO of the anticuboctahedral Pd_{13} core does not have a symmetry of inversion but that of the cuboctahedral Pd_{13} has it. Because the d orbital of the Pd^C atom has a symmetry of inversion, the d orbital of the Pd^C atom participates in the HOMO of the cuboctahedral Pd_{13} core in an antibonding way but does not in the HOMO of the anticuboctahedral Pd_{13}. Consequently, the HOMOs exist at a higher energy in the cuboctahedral Pd_{13} core than in the anticuboctahedral one. In addition, the cuboctahedral Pd_{13} core has triply-degenerated HOMOs but the anticuboctahedral Pd_{13} has a non-degenerated HOMO (Fig. 4a). Because of these features of the HOMO, the CT from the Pd_{13} core to the $[(C_7H_7)_6]^{2+}$ ligand shell is stronger in **Cubo-μ4** than in **Anti-μ4**; additional discussion of HOMO-1 and HOMO-2 is presented in Scheme S5 of the ESI.

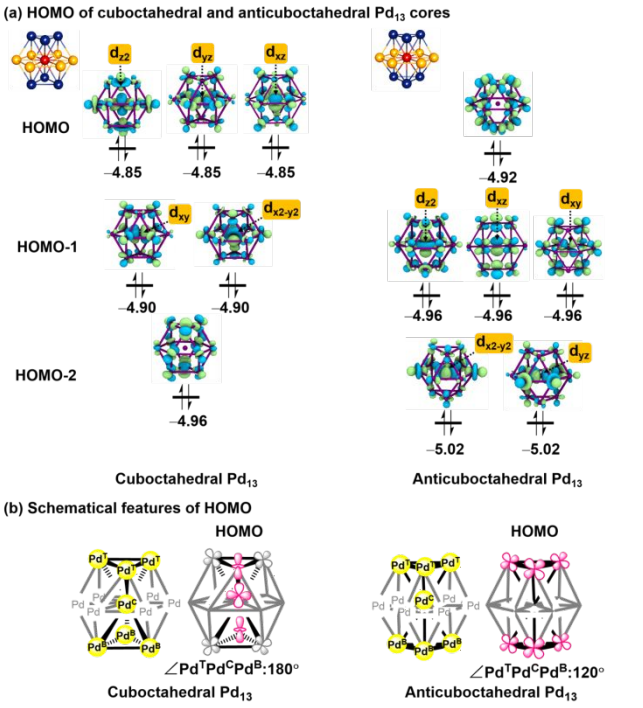

Fig. 4. The HOMOs of cuboctahedral and anti-cuboctahedral Pd_{13} clusters (a) and their schematical features (b). The optimized geometries of cuboctahedral and anti-cuboctahedral Pd_{13} clusters were employed. Orbital energies are presented in eV unit.

One more factor is the steric repulsion between three μ_4-C_7H_7 ligands interacting with the upper part of the Pd_{13} core and three μ_4-C_7H_7 ligands interacting with the lower part. As shown in Scheme 4a, three μ_4-C_7H_7 ligands on the upper part are distant from three μ_4-C_7H_7 ligands on the lower part in **Cubo-μ4** because three Pd_4 planes of the upper part are distant from three Pd_4 planes of the lower part. In **Anti-μ4**, however, three μ_4-C_7H_7 ligands on the upper part are

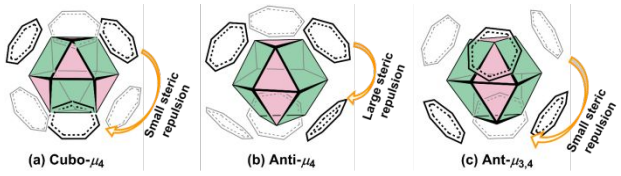

Scheme 4. Schematical picture showing the positions of μ_3- and μ_4-C_7H_7 ligands.

close to three μ_4-C_7H_7 ligands on the lower part because three Pd_4 planes of the upper part exist at the positions neighbouring to three Pd_4 planes of the lower part (Scheme 4b). Consequently, the steric repulsion between the upper μ_4-C_7H_7 and the lower μ_4-C_7H_7 ligands is large in **Anti-μ4**. Because of the steric repulsion in **Anti-μ4**, μ_4-C_7H_7 ligands are not located at the best position to interact with the Pd_{13} core, leading to the presence of the small E_{int} value.

It is concluded that the cuboctahedral Pd_{13} core is better than the anticuboctahedral Pd_{13} core for the formation of six μ_4-coordination bonds with the C_7H_7 ligands in both the electronic and steric factors.

Comparison between Cubo-μ4 with μ_4-C_7H_7 coordination bonds and Cubo-μ3 with μ_3-ones. Here, we compare **Cubo-μ4** and **Cubo-μ3**. This comparison is the same as that between the μ_4-coordination bond of C_7H_7 in **Cubo-μ4** and the μ_3-one in **Cubo-μ3**. As shown in Table 2, the E_{int} value is much more negative in **Cubo-μ4** than in **Cubo-μ3**, indicating that the μ_4-coordination bond of the C_7H_7 ligand is much stronger than the μ_3-one. The stronger μ_4-coordination bond is one of important factors to stabilize **Cubo-μ4** compared to the other isomers possessing the μ_3-coordination bonds. Therefore, it is crucially important to elucidate the reason.

In **Cubo-μ4**, each Pd atom of the upper Pd_3 plane participates in two neighbouring Pd_4 planes (Fig. 2a). This means that one Pd atom of the Pd_3 plane interacts with two μ_4-C_7H_7 molecules, as shown in Scheme 4a. Because such an interaction structure seems congested, we checked whether the interaction structure is congested or not. As shown in the top view of Fig. 5a, each Pd atom of the upper Pd_3 plane can interact with two C=C double bonds of two C_7H_7 molecules and each C_7H_7 ligand interacts with two Pd atoms belonging to the top Pd_3 plane using two C=C double bonds. This interaction structure seems reasonable. As shown in the side-view of Fig. 5a, two C=C double bonds of one C_7H_7 ligand interact with two Pd atoms belonging to the Pd_3 plane and the remaining three C atoms interact with two Pd atoms belonging to the equatorial Pd_6 plane. The latter interaction structure resembles a π-allyl group bridging two Pd atoms. In this interaction, the two C-C bonds have almost the same distance (1.426 Å and 1.425 Å; Top view of Fig. 5a) but the two Pd-C bond distances differ moderately from each other (2.166 Å and 2.197 Å; the side-view of Fig. 5a).[§6] These features indicate that the μ_4-coordination bond is formed without any constraint in **Cubo-μ4**.

In the μ_3-coordination bond of C_7H_7 of **Cubo-μ3**, each Pd atom of the upper Pd_3 plane interacts with one C=C double bond of one C_7H_7 molecule (top-view in Fig. 5b). This structure is not congested, indicating that three Pd atoms of the Pd_3 plane interact with three C_7H_7 ligands without any constraint. The side-view of Fig. 5b shows that one C=C double bond of C_7H_7 interacts with one Pd atom belonging to the Pd_3 plane and the other three C atoms interact with two Pd atoms belonging to the equatorial Pd_6 plane. The latter interaction resembles a π-allyl group bridging two Pd atoms like in the μ_4-coordination of **Cubo-μ4**. However, the remaining two C atoms of C_7H_7 cannot find any Pd atom for interaction partner (side view of Fig. 5b) in contrast with the μ_4-coordination case in which all seven C atoms of C_7H_7 can interact with four Pd atoms of the Pd_4 plane (the side-view of Fig. 5a). Therefore, the μ_4-coordination bond of C_7H_7 is stronger than the μ_3-one. Indeed, the interaction energy of

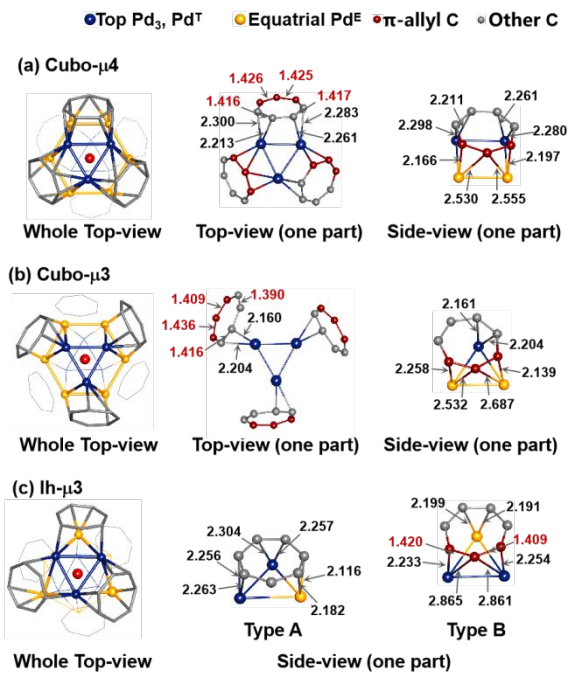

Fig. 5 Interaction structures of the μ_4- and μ_3-coordinations of C_7H_7 in **Cubo-μ4** (a), **Cubo-μ3** (b) and **Ih-μ3** (c). Numbers represent bond distance in angstrom (Å) unit.

one C_7H_7 molecule is larger in **Cubo-μ4** than in **Cubo-μ3** by 12.9 kcal/mol[§7] (Table 2).

The stronger μ_4-coordiantion bond than the μ_3-one is consistent with such properties as the larger HOMO-LUMO energy gap in **Cubo-μ4** than in **Cubo-μ3** (Figs. 3a and 3c), the less positively charged C_7H_7 in **Cubo-μ4** than in **Cubo-μ3** (Fig. 2) and the shorter $R(Pd^C–X)$ distance in **Cubo-μ4** than in **Cubo-μ3** (Table 1).

Comparison between Cubo-μ4 and Ih-μ3. Ih-μ3 is much more unstable than the most stable **Cubo-μ4** by 41.3 kcal/mol in the total energy and 38.5 kcal/mol in the Gibbs energy (Fig. 2) despite that the icosahedral Pd_{13} cluster is the most stable (Fig. 1) and both the Pd_{13} core and the $[(C_7H_7)_6]^{2+}$ ligand shell in **Ih-μ3** are more stable than in **Cubo-μ4** (Table 2). The larger stability of **Cubo-μ4** than **Ih-μ3** results from the considerably larger (more negative) E_{int} value in **Cubo-μ4** than in **Ih-μ3**.

Because the icosahedral Pd_{13} core exposes the Pd_3 planes to the surface but no Pd_4 plane, all the C_7H_7 molecules must interact with the Pd_3 planes in **Ih-μ3**. In **Ih-μ3**, two kinds of μ_3-C_7H_7 coordination structure are found. In one μ_3-C_7H_7 coordination bond (Type A in Fig. 5c), three C=C double bonds interact with three Pd atoms but one C atom cannot interact with any Pd atom. In the other μ_3-C_7H_7 coordination bond (Type B in Fig. 5c), one C=C double bond coordinates to one Pd atom, three C atoms coordinate to two Pd atoms through a π-allyl type interaction but two remaining C atoms cannot interact with any Pd atom. Because seven C atoms of C_7H_7 can interact with Pd atoms in the μ_4-coordination bond, it is concluded that both type A and B μ_3-coordination bonds of C_7H_7 in **Ih-μ3** are

weaker than the μ_4-coordination bonds in **Cubo-μ4**. This result is consistent with the more positive charge (0.225 *e*; Fig. 2) of the μ_3-C_7H_7 ligand and the longer $R(Pd^C–X)$ distance (2.202 Å; Table 1) in **Ih-μ3** than those of **Cubo-μ4**. Therefore, the E_{int} value of **Ih-μ3** is smaller than that of **Cubo-μ4**. This is the reason why **Ih-μ3** is less stable than **Cubo-μ4**.

Comparisons between **Anti-μ4** and **Anti-μ3,4** and between **Ih-μ3** and **Cubo-μ3** are discussed in the ESI (p. S13) because these comparisons do not directly relate to the most stable **Cubo-μ4**: Here, we wish to mention that **Anti-μ3,4** is more stable than **Anti-μ4** because the μ_4-coordination bond of C_7H_7 in **Anti-μ3,4** is stronger than that of **Anti-μ4** due to the smaller steric repulsion, as shown in Schemes 4b and 4c.

Conclusions

This work systematically investigated nano-scale Pd_{13} cluster complexes with cuboctahedral, anticuboctahedral and icosahedral Pd_{13} cores surrounded by six cyclic π electron ligands using DFT calculations. Important findings are summarized below: **Cubo-μ4** is much more stable than isomers such as **Cubo-μ3**, **Anti-μ4**, **Anti-μ3,4** and **Ih-μ3**. This result is consistent with the experimental observation that only **Cubo-μ4** was obtained but the other isomers were not, which is the answer to the question (i). The key factor governing the relative stabilities of these Pd_{13} cluster complexes is not the stability of the Pd_{13} core but the interaction energy E_{int} between the Pd_{13} core and the $[(C_7H_7)_6]^{2+}$ ligand shell, which is the question (ii). This is the first knowledge of the key factor, whereas we have to remind that the key factor may depend on the kinds of metal and ligand. The E_{int} value is determined by the HOMO of the Pd_{13} core and the C_7H_7 coordination mode because the CT occurs from the Pd_{13} core to the $[(C_7H_7)_6]^{2+}$ ligand shell and the μ_4-coordination bond is stronger than the μ_3-one, as described below. Although all the seven C atoms of C_7H_7 can interact with the Pd_4 plane in the μ_4-coordination bond, one or two C atoms of C_7H_7 cannot interact with the Pd atom in the μ_3-one. Thus, the μ_4-coordination bond of C_7H_7 is stronger than the μ_3-one and the C_7H_7 ligand coordinates to the Pd_4 plane when the Pd_{13} core has Pd_4 planes, which is the answer to the question (iii). For analysing relative stabilities of these Pd cluster complexes, we separated the Pd cluster complex into the Pd_{13} core and the $[(C_7H_7)_6]^{2+}$ ligand shell and discussed the stability using stabilization energies of the Pd_{13} core and the ligand shell and the interaction energy E_{int} between them. This method is effective for investigating Pd_{13} cluster complexes, which is the question (iv).

Comparison of **Cubo-μ4** with other isomers is summarized in Scheme 5. As shown in Scheme 5a, the icosahedral Pd_{13} core has a non-degenerated HOMO at the highest energy, the cuboctahedral Pd_{13} core has triply-degenerated HOMOs at a medium energy and the anticuboctahedral Pd_{13} core has a non-degenerated HOMO at the lowest energy. The cuboctahedral Pd_{13} core has three Pd_4 planes in the upper part of the Pd_{13} core at distant positions from three Pd_4 planes in the lower part, but the anticuboctahedral Pd_{13} core has three Pd_4 planes in the upper part at the positions neighbouring to the Pd_4 planes in the lower part. Because CT occurs from the Pd_{13} core to the $[(C_7H_7)_6]^{2+}$ ligand shell, **Cubo-μ4** is better than **Anti-μ4** from the electronic factor (HOMO energy) and the steric factor, as follow: In **Cubo-μ4**, the C_7H_7 ligands can form the strong μ_4-coordination bonds with the Pd_{13} core because the triply-degenerated HOMOs exist at a medium energy in the cuboctahedral Pd_{13} core and the steric repulsion between C_7H_7 ligands is small. In **Anti-μ4**, the μ_4-coordination bonds of the six C_7H_7 ligands are weak because the non-degenerated HOMO exists at the lowest energy and the steric repulsion between C_7H_7 ligands is large. As compared in Scheme 5b, the μ_4-coordination bond is stronger than the μ_3-one. The icosahedral Pd_{13} core has Pd_3 planes but no Pd_4 plane. Consequently, **Ih-μ3** is not good despite the presence of the HOMO at the highest energy. **Ant-μ3,4** is better than **Anti-μ4** because the steric repulsion between μ_4-C_7H_7 and μ_3-C_7H_7 ligands is smaller and the μ_4-C_7H_7 coordination bond is stronger in **Ant-μ3,4** than in **Anti-μ4**. However, **Ant-μ3,4** is not good compared to **Cubo-μ4** because **Anti-μ3,4** has three μ_3-C_7H_7 coordination bonds but **Cubo-μ4** has six

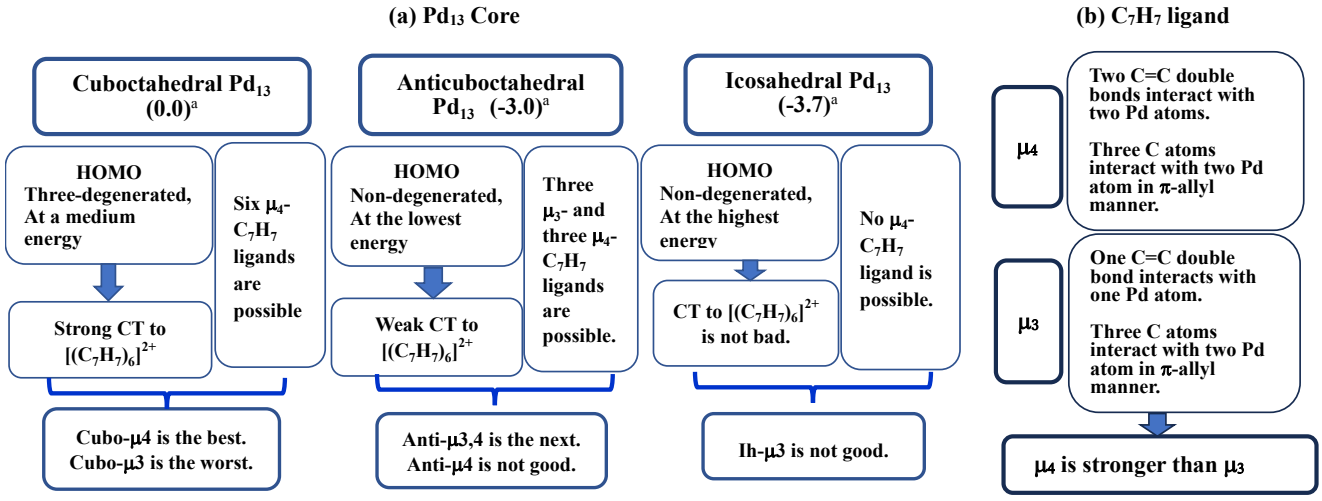

Scheme 5. Summaries of cuboctahedral, anticuboctahedral and icosahedral Pd_{13} cores (A) and the interaction between the Pd_{13} core and C_7H_7 ligands (B). [a]Numbers are relative energy of Pd_{13} cluster without ligand (in kcal/mol unit).

μ_4-C_7H_7 coordination bonds. Therefore, **Cubo-μ4** is the most stable in these Pd_{13} cluster complexes.

At the last, we wish to state that the analysis using the stabilization energies of the Pd_{13} core and the ligand shell and the interaction energy between them is one of effective methods to investigate the structures and stabilities of the Pd_{13} cluster complexes. This analysis method can be applied to other metal cluster complexes.

Computational details and models

DFT calculations were carried out using the B3PW91 functional[29-33] with the Grimme's empirical dispersion correction (D3)[34,35] and the Becke-Johnson (BJ) damping function.[36-38] Geometry optimizations were performed in gas phase, using LANL2DZ basis set[39] for valence electrons of Pd atom with the corresponding effective core potentials (ECPs) for its core electrons and the 6-31G(d) basis sets for other atoms (H and C). This basis set system is named BS-I in this work. Frequency calculations were performed at the B3PW91-D3(BJ)/BS-I level to make sure that the optimized geometry does not have any imaginary frequency. The optimized geometry of **Cubo-μ4** is in good agreement with the experimental one, considering the large size and flexible structure of the Pd_{13} cluster complex, as shown by Table S1 of the ESI and brief discussion there.[§]

We further performed single-point calculations using the geometries optimized above to obtain better relative stabilities and electronic structures, where the Stuttgart-Dresden-Bonn (SDB) basis set[40,41] was used for valence electrons of Pd atom with the corresponding ECPs for its core electrons and 6-311G(d) basis sets were used for other atoms. This basis set system is named BS-II. The SMD (solvation model based on solute electron density)[42] was used in the single-point calculations to evaluate the solvation effects of dichloromethane. After making comparison between the NBO charge[28] and the Hirshfeld charge,[27] we selected the Hirshfeld charge for discussion in this work because the NBO charge of the centre Pd atom of **Cubo-μ4** seems overly negative, as shown in Table S2 of the ESI, where we employed version 7 of NBO analysis.[43] Considering the definition,[27] it is likely that the Hirshfeld charge is reasonable to discuss atomic charge of metal clusters/particles. These calculations were carried out using Gaussian16 program.[44]

We analysed relative stabilities of **Cubo-μ4** and isomers by separating the Pd cluster complex into the Pd_{13} core and the $[(C_7H_7)_6]^{2+}$ ligand shell. This method is essentially the same as the energy decomposition analysis of intermolecular interaction[45,46] and the distortion/interaction analysis of transition state.[47,48] In this regard, the analysis method is not special but has not been applied to nano-scale metal cluster complexes to our knowledge.

Although $[Pd_{13}(\mu_4\text{-}C_7H_7)_6][B(Ar^F)_4]_2$ {Ar^F = 3,5-$(CF_3)_2(C_6H_3)$} was experimentally obtained, the $[Pd_{13}(\mu_4\text{-}C_7H_7)_6]^{2+}$ moiety without $[B(Ar^F)_4]^-$ anions was employed for calculation because the counter anions do not interact strongly with the $[Pd_{13}(\mu_4\text{-}C_7H_7)_6]^{2+}$ moiety. The structure of **Anti-μ4** was constructed from that of **Cubo-μ4** by rotating the bottom Pd_3 plane of **Cubo-μ4** by 60°; see Fig. 1 for cuboctahedral Pd_{13} and anti-cuboctahedral Pd_{13} structures. Then, we optimized its geometry with six μ_4-coordinated C_7H_7 ligands. The structure of **Anti-μ3,4** was constructed starting from that of **Anti-μ4** by replacing three upper μ_4-C_7H_7 ligands with three μ_3-C_7H_7 ligands. Although the structure of **Anti-μ3** with six μ_3-C_7H_7 ligands was constructed in a similar manner, this geometry could not be optimized because this structure automatically changed to **Anti-μ3,4** during the geometry optimization. The structure of **Ih-μ3** was constructed by combining the optimized icosahedral Pd_{13} core with six μ_3-C_7H_7 molecules; note that only μ_3-coordination is possible in the icosahedral Pd_{13} case because the icosahedral Pd_{13} core exposes Pd_3 planes to the surface but no Pd_4 plane. In this model, we placed C_7H_7 molecules on the Pd_{13} surface as distant as possible from each other.

Author Contributions

B. Z. performed all the calculations, made figures, tables, schemes, and analysis of computational results.

T. M. provided motivation and made story of discussion, analysis and explanation of results.

S. S. proposed almost all research plan and made most of analysis, and presented almost all explanations and discussions.

Conflicts of interest

There are no conflicts to declare.

Acknowledgements

This work was supported by JST-CREST (JPMJCR20B6), JSPS Grant-in-aid for Scientific Research (JP22H02093), Mitsubishi Foundation. B. Z. is grateful to the National Science Fund in China (NSFC 22203014). We wish to thank Research Centre for Computational Science in National Institutes of Natural Sciences (NINS), Okazaki, Japan for the use of Super Computers (Project: 22-IMS-C003 and 23-IMS-C003).

Notes and references

[§]The difference between the longest Pd-Pd distance and the shortest one of the optimized structure is somewhat larger than that of the experimental one. Considering the large size of **Cubo-μ4**, flexibility of the Pd_{13} core and the easily mobile position and orientation of the C_7H_7 ligands, however, this is not a very poor result. Indeed, this is better than the previously calculated value.[19]

[§2]Here, we discuss this issue separating Pd nuclear charges and electron density. The nuclear charges of thirteen Pd atoms provide the largest electrostatic potential at the Pd^C atom. Consequently, the electron density tends to accumulate there, simply thinking. If we think Pd nuclei with 46 electrons, the similar discussion is possible, as follows: Because the Pd nuclear charge is not completely shielded by 46 electrons, the neutral Pd atom exhibits electrostatic potential withdrawing electron density. Such electrostatic potential is the largest at the Pd^C atom because this position is surrounded by twelve Pd atoms but the Pd^S atom is not perfectly surrounded by Pd atoms. Thus, the electron density tends to accumulate on the Pd^C atom.

[§3]At this moment, however, we do not have a clear explanation why the WBI value of the Pd^C-Pd^S bond is larger than that of the Pd^S-Pd^S bond.

[§4]Because the Hirshfeld analysis methof[27] tends to present a smaller absolute value of charge than the NBO analysis method,[28] we also evaluated the NBO charge of each C_7H_7 ligand in **Cubo-μ4** and found that the NBO charge is −0.274 *e* (Table S2 of the Supporting Information). This value differs very much from the formal positive charge of the tropylium cation, indicating that it is not reasonable to understand that the C_7H_7 ligand is a tropylium cation in **Cubo-μ4**.

[§5]Here, we compared HOMO energy using the optimized Pd_{13} bare cluster because the Pd_{13} cores in **Cubo-μ4** and **Anti-μ4** distort and the HOMO energy is influenced by the distortion. In other words, the discussion is presented on the intrinsic ability of HOMO of the Pd_{13} cluster for the CT from the Pd_{13} core to the $[(C_7H_7)_6]^{2+}$ ligand shell.

[§6]This difference between two Pd-C bond distances suggests that the π-allyl structure moderately deviates from the symmetrical π-allyl structure toward the σ-allyl type structure. This is consistent with the experimental report.[18]

[§7]This value (12.9 kcal/mol) is obtained from Table 2, as follows: The difference in E_{int} between **Cubo-μ4** and **Cubo-μ3** is 77.5 kcal/mol. These Pd cluster complexes have six coordination bonds with the C_7H_7 ligand. Therefore, the difference in stabilization energy by one C_7H_7 coordination is 12.9 kcal/mol (= 77.5/6); in other words, this is an average value.

1 E. Roduner, *Chem. Soc. Rev.*, 2006, **35**, 583-592.
2 S. Cao, F. F. Tao, Y. Tang, Y. Li and J. Yu, *Chem. Soc. Rev.*, 2016, **45**, 4747-4765.
3 L. Liu and A. Corma, *Chem. Rev.*, 2018, **118**, 4981-5079.
4 T. Ishida, T. Murayama, A. Taketoshi and M. Haruta, *Chem. Rev.*, 2020, **120**, 464-525.
5 P. J. Dyson and J. S. McIndoe, *Transition Metal Carbonyl Cluster Chemistry*, the Gordon and Breach Science Publishers (2000).
6 P. J. Dyson, *Coord. Chem. Rev.*, 2004, **248**, 2443-2458.
7 M. S. Paquette and L. F. Dahl, *J. Am. Chem. Soc.*, 1980, **102**, 6623-6626.
8 W. Buchowicz, B. Herbaczynska, L. B. Jerzykiewicz, T. Lis, S. Pasynkiewicz and A. Pietrzykowski, *Inorg. Chem.*, 2012, **51**, 8292-8297.
9 Y. Ohki, N. Uehara and H. Suzuki, *Organometallics*, 2003, **22**, 59-64.
10 K. Yamamoto, T. Sugawa and T. Murahashi, *Coord. Chem. Rev.*, 2022, **466**, 214575.
11 T. Murahashi, M. Fujimoto, Y. Kawabata, R. Inoue, S. Ogoshi and H. Kurosawa, *Angew. Chem. Int. Ed.*, 2007, **119**, 5536-5539.
12 T. Murahashi, K. Usui, R. Inoue, S. Ogoshi and H. Kurosawa, *Chem. Sci.*, 2011, **2**, 117-122.
13 T. Murahashi, K. Usui, Y. Tachibana, S. Kimura and S. Ogoshi, *Chem. Eur. J.*, 2012, **18**, 8886-8890.
14 Y. Ishikawa, S. Kimura, K. Takase, K. Yamamoto, Y. Kurashige, T. Yanai and T. Murahashi, *Angew. Chem. Int. Ed.*, 2015, **54**, 2482-2486.
15 Y. Ishikawa, S. Kimura, K. Yamamoto and T. Murahashi, *Chem. Eur. J.*, 2017, **23**, 14149-14152.
16 T. Murahashi, M. Fujimoto, M. Oka, Y. Hashimoto, T. Uemura, Y. Tatsumi, Y. Nakao, A. Ikeda, S. Sakaki and H. Kurosawa, *Science*, 2006, **313**, 1104-1107.
17 S. Horiuchi, Y. Tachibana, M. Yamashita, K. Yamamoto, K. Masai, K. Takase, T. Matsutani, S. Kawamata, Y. Kurashige, T. Yanai and T. Murahashi, *Nat. Commun.*, 2015, **6**, 6742.
18 M. Teramoto, K. Iwata, H. Yamaura, K. Kurashima, K. Miyazawa, Y. Kurashige, K. Yamamoto and T. Murahashi, *J. Am. Chem. Soc.*, 2018, **140**, 12682-12686.
19 J. Wei, S. Kahlal, J.-F. Halet and J.-Y. Saillard, *J. Cluster Science*, 2019, **30**, 1227-1233.
20 W. D. Knight, *Phys. Rev. Lett.*,1984, **52**, 2141-2143.
21 W. A. de Heer, *Rev. Mod. Phys.*, 1993, **65**, 611-676.
22 K. Wade, *J. Chem. Soc. D*, 1971, 792–793.
23 K. Wade, *Adv. Inorg. Chem. Radiochem.*, 1976, **18**, 1–66.
24 D. M. P. Mingos, *Nat. Phys. Sci.*, 1972, **236**, 99–102.
25 D. M. P. Mingos, *Acc. Chem. Res.,* 1984, **17**, 311–319.
26 K. B. Wiberg, *Tetrahedron*, 1968, **24**, 1083-1096.
27 F. L. Hirshfeld, *Theor. Chem. Acc.,* 1977, **44**, 129-38.
28 A. E. Reed, L. A. Curtiss and F. Weinhold, *Chem. Rev.*, 1988, **88**, 899-926.
29 A. D. Becke, *Phys. Rev. A*, 1988, **38**, 3098-3100.
30 A. D.Becke, *J. Chem. Phys.*, 1993, **98**, 5648-5652.
31 J. P. Perdew, J. A. Chevary, S. H. Vosko, K. A. Jackson, M. R. Pederson, D. J. Singh and C. Fiolhais, *Phys. Rev. B: Condens. Matter Mater. Phys.*, 1992, **46**, 6671-6687.
32 J. P. Perdew, J. A. Chevary, S. H. Vosko, K. A. Jackson, M. R. Pederson, D. J. Singh and C. Fiolhais, *Phys. Rev. B: Condens. Matter Mater. Phys.*, 1993, **48**, 4978-4990.
33 J. P. Perdew, K.Burke and Y. Wang, *Phys. Rev. B: Condens. Matter Mater. Phys*, 1996, **54**, 16533-16539.
34 S. Grimme, J. Antony, S. Ehrlich and H. Krieg, *J. Chem. Phys.*, 2010, **132**, 154104.
35 U. Ryde, R. A. Mata and S. Grimme, *Dalton Trans.*, 2011, **40**, 11176-11183.
36 A. D. Becke and E. R. Johnson, *J. Chem. Phys.*, 2005, **123**, 154101.
37 A. D. Becke and E. R. Johnson, *J. Chem. Phys.*, 2007, **127**, 154108.
38 E. R. Johnson and A. D. Becke, *J. Chem. Phys.*, 2006, **124**, 174104.
39 P. J. Hay and W. R. Wadt, *J. Chem. Phys*., 1985, **82**, 299-310.
40 M. Dolg, U. Wedig, H. Stoll and H. J. Preuss, *J. Chem. Phys.*, 1987, **86**, 866-872.
41 J. M. L Martin and A. J. Sundermann, *J. Chem. Phys*., 2001, **114**, 3408-3420.
42 A. V. Marenich, C. J. Cramer, and D. G. Truhlar, *J. Phys. Chem. B*, 2009, **113**, 6378-6396.
43 E. D. Glendening, J. K. Badenhoop, A. E. Reed, J. E. Carpenter, J. A. Bohmann, C. M. Morales, C. R. Landis and F. Weinhold, NBO 6.0, Theoretical Chemistry Institute, University of Wisconsin, Madison, WI, 2013; http://nbo6.chem.wisc.edu/.
44 M. J. Frisch, G. W. Trucks, H. B. Schlegel, G. E. Scuseria, M. A. Robb, J. R. C. heeseman, G. Scalmani, V. Barone, B. Mennucci, G. A. Petersson, H. Nakatsuji, et al. *Gaussian 16*, Revision C.01, Gaussian, Inc.: Wallingford CT, 2016.
45 K. Kitaura and K. Morokuma, *Int. J. Quant. Chem*. 1976, **10**, 325-340.
46 H. Umeyama and K. Morokuma, *J. Am. Chem. Soc.*, 1976, **98**, 7208-7220.
47 D. H. Ess and K. N. Houk, *J. Am. Chem. Soc.* 2007, **129**, 10646-10647.
48 F. M. Bickelhaupt and K. N. Houk. *Angew. Chem. Int. Ed*. 2017, **56**, 10070–10086.